

Electronic Supporting Information (ESI) for

Highly interconnected ordered mesoporous carbon – carbon nanotube nanocomposites: Pt-free, highly efficient, and durable counter electrode for dye-sensitized solar cells

Yimhyun Jo,^{‡^a} Jae Yeong Cheon,^{‡^b} Jeonghun Yu,^a Hu Young Jeong,^c Chi-Hwan Han,^a Yongseok Jun*^a and Sang Hoon Joo*^b

^a *Interdisciplinary School of Green Energy and KIER-UNIST Advanced Center for Energy, Ulsan National Institute of Science and Technology (UNIST), Ulsan 689-798, Republic of Korea. E-mail: yjun@unist.ac.kr*

^b *School of Nano-Bioscience and Chemical Engineering, KIER-UNIST Advanced Center for Energy, and Low Dimensional Carbon Materials Center, Ulsan National Institute of Science and Engineering (UNIST), Ulsan 689-798, Republic of Korea. E-mail: shjoo@unist.ac.kr; Fax: +82 52 217 2509; Tel: +82 52 217 2522*

^c *UNIST Central Reserach Facility and School of Mechanical and Advanced Materials Engineering, Ulsan National Institute of Science and Technology (UNIST), Ulsan 689-798, Republic of Korea.*

[‡] These authors contributed equally to this work.

Experimental Details

Synthesis of OMC–CNT nanocomposites: A hexagonally ordered OMS template was synthesized following the literature method for SBA-15 silica¹ with the modification of hydrothermal treatment temperature at 150°C. The OMC–CNT nanocomposites were synthesized by a solid state nanocasting method using OMS and Ni-phthalocyanine (NiPc, Aldrich) as a template and as a precursor, respectively.² 1.0 g of calcined OMS was mixed with 1 g of NiPc, and the mixture was grinded for 10 min in a mortar and transferred to an alumina crucible. The mixture was then heated to 900°C with a ramping rate of 2.5°C min⁻¹ and remained at that temperature for 3 h under Ar flow. The resulting carbon-silica composite was then washed twice with hydrofluoric acid (50 wt%, J.T.Baker) at room temperature for 1 h to remove the OMS template. The synthesis of OMC was achieved using the same procedure as that for the OMC–CNT nanocomposites, except for the use of phthalocyanine (Pc, Aldrich) as the carbon precursor.

DSSC tests: FTO glass (TEC-8, Pilkington) was cleaned by sonicating in ethanol, acetone, and then isopropanol for 10 min and UV exposure for 20 min. A Doctor blade process was applied to evenly apply TiO₂ paste (ENB Korea, 20 nm) on cleaned FTO glass with a thickness of around 12 μm, and the sample was subsequently sintered at 500°C for 80 min. TiCl₄ treatment was carried out by placing the sample in 40 mM TiCl₄ aqueous solution for 30 min followed by sintering at 500°C again for 30 min. Dye coating was performed in 0.3 mM of N719 solution in acetonitrile/ter-buthanol (1:1 vol.) for overnight. The counter electrode (CE) was prepared with materials of interest. For a reference, CE with Pt was prepared by spin-coating (2000 rpm, 5 times) 20 mM of H₂PtCl₆ solution in isopropanol on FTO glass 5 times and sintering at 400°C for 1 h. For the OMC–CNT nanocomposites and

OMC, each material was dispersed in an organic vehicle (2-methoxy-ethanol), and an ultrasonic disperser (Sonics, 750) was applied for 5 min, and composition ratio was set at 1:100 (wt %). The mixture was loaded on FTO glass by spin-coating (1500 rpm, 3 times, 1 μm) and sintering at 400°C under Ar condition. Finally, the electrodes were assembled, and an electrolyte was added through a pre-drilled hole. The hole was sealed with Surlyn and a piece of thin glass. The composition of the electrolyte was 0.5 M 1-hexyl-2,3-dimethylimidazolium iodide (99.9%, C-tri), 0.02 M iodine (ACS reagent, Aldrich), 0.5 M 4-tert-butylpyridine (Aldrich), and 0.05 M lithium iodide (Aldrich) in acetonitrile. *J-V* characterization was carried out under 1 Sun condition with Oriel SOL3A solar simulator by obtaining open circuit voltage (V_{oc}), short circuit current (J_{sc}), fill factor (FF), and overall efficiency (η).

Electrochemical and physicochemical characterizations: Electrochemical impedance spectroscopy (EIS) and cyclic voltammetry (CV) were completed with Solartron. For CV, Ag/AgNO₃ and Pt mesh were used as a reference electrode and counter electrode, respectively. The electrolyte for CV was prepared with 1 mM I₂, 10 mM Lithium iodide, and 100 mM LiClO₄ in N₂ purged acetonitrile, and the scan rate was 100 mV/s. Morphology of the samples was analyzed by scanning electron microscope (SEM) using a FEI Quanta 200 microscope operating at 15 kV, whereas internal pore structures were visualized by transmission electron microscope (TEM) images using a JEOL JEM-2100F microscope at an accelerating voltage of 200 kV. X-ray diffraction (XRD) patterns of the samples were measured with a Rigaku D/Max 2500V/PC X-ray diffractometer equipped with a Cu K α source at 40 kV and 200 mA. Porous structures of the samples were analyzed by nitrogen adsorption at -196°C using a BEL Belsorp-Max machine. Surface areas and pore size distributions of the samples were calculated by using the Brunauer-Emmett-Teller (BET) equation and the Barrett-Joyner-

Halenda (BJH) method, respectively. The carbon and nitrogen contents in the samples were determined by Thermo Scientific Flash 2000 elemental analyzer. Themogravimetric analysis (TGA) was conducted in air and argon atmospheres at a heating rate of $10^{\circ}\text{Cmin}^{-1}$, using a TA Hi-Res TGA 2950 thermogravimetric analyzer.

References

1. D. Zhao, J. Feng, Q. Huo, N. Melosh, G. H. Fredrickson, B. F. Chmelka and G. D. Stucky, *Science*, 1998, **279**, 548–552.
2. K. T. Lee, X. Ji, M. Rault and L. F. Nazar, *Angew. Chem., Int. Ed.* 2009, **48**, 5661–5665.

Table S1 Photovoltaic parameters for DSSCs employing different counter electrodes and EIS parameters of dummy cells assembled from these electrodes.^[a]

Sample	V_{oc} (V)	J_{sc} (mA cm ⁻²)	FF (%)	η (%)	R_{ct} (Ω cm ²)	Z_w (Ω cm ²)	R_s (Ω cm ²)
OMC–CNT	0.749	16.2	69.1	8.4	1.37	7.47	0.74
OMC	0.744	16.0	55.9	6.7	52.75	43.56	1.01
CNT	0.719	14.7	38.0	4.0	2.49	17.01	0.94
Pt	0.749	16.1	68.7	8.3	1.40	6.85	0.68

[a] V_{oc} : open circuit voltage, J_{sc} : short circuit current, FF: fill factor, η : cell efficiency, R_{ct} : charge transfer resistance, Z_w : diffusion impedance, and R_s : ohmic internal resistance

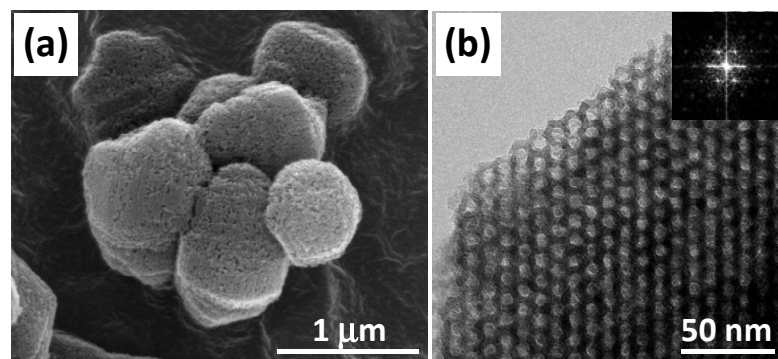


Fig. S1 (a) SEM and (b) TEM images of OMS template.

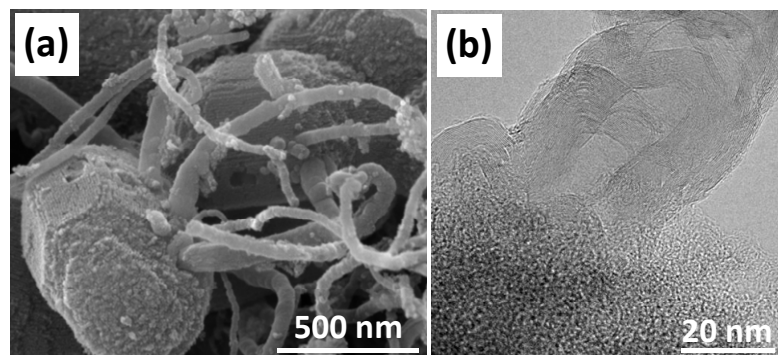


Fig. S2 High magnification (a) SEM and (b) TEM images of OMC-CNT nanocomposites.

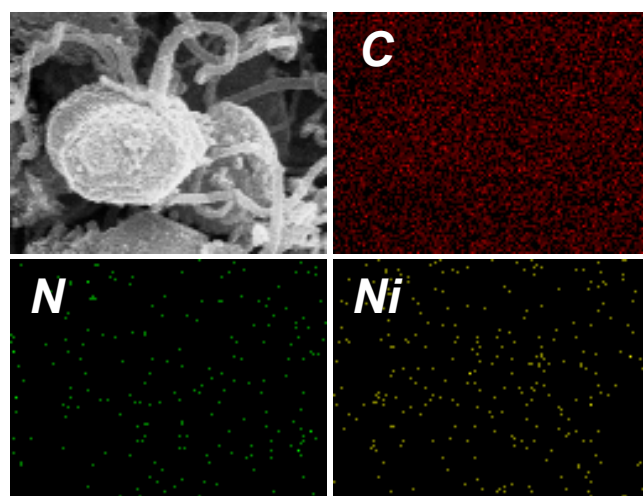


Fig. S3 Energy dispersive X-ray spectroscopy analysis of OMC–CNT.

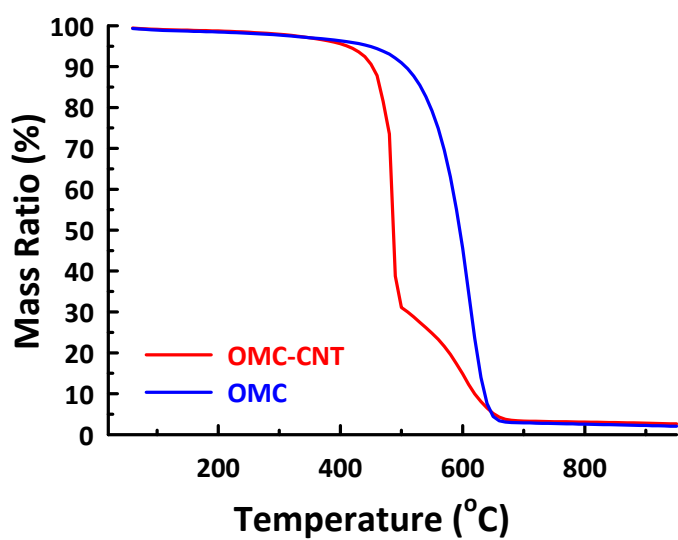


Fig. S4 Thermogravimetric analysis of OMC–CNT and OMC samples.

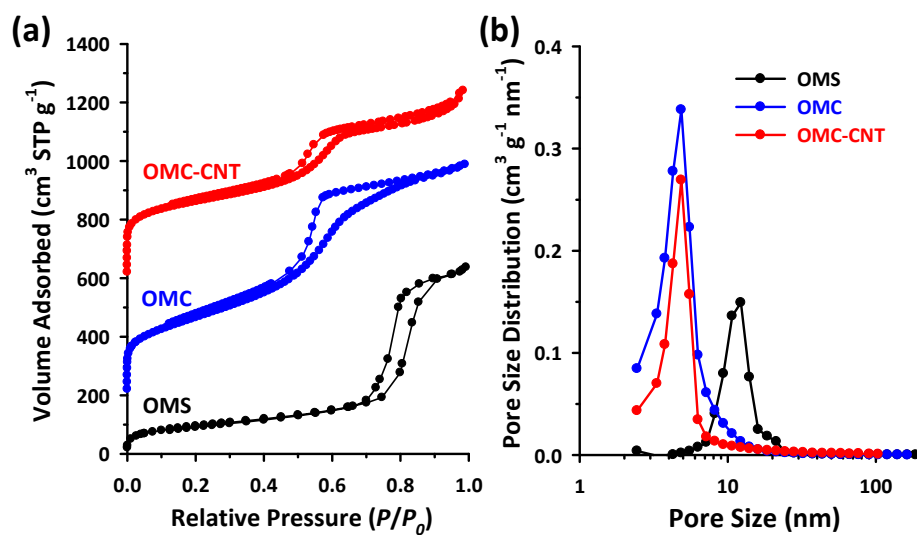


Fig. S5 (a) nitrogen adsorption isotherms and (b) pore size distributions of OMS, OMC, and OMC-CNT samples. In (a), isotherms of OMC and OMC-CNT samples were shifted upwards 200 and 600 $\text{cm}^3 \text{g}^{-1}$, respectively, for clarity.

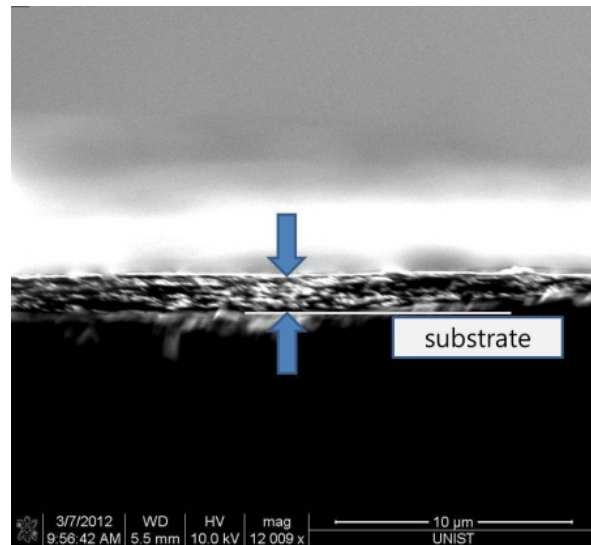


Fig. S6 SEM image of OMC-CNT counter electrode. The thickness of active layer is about 1.5 μm .

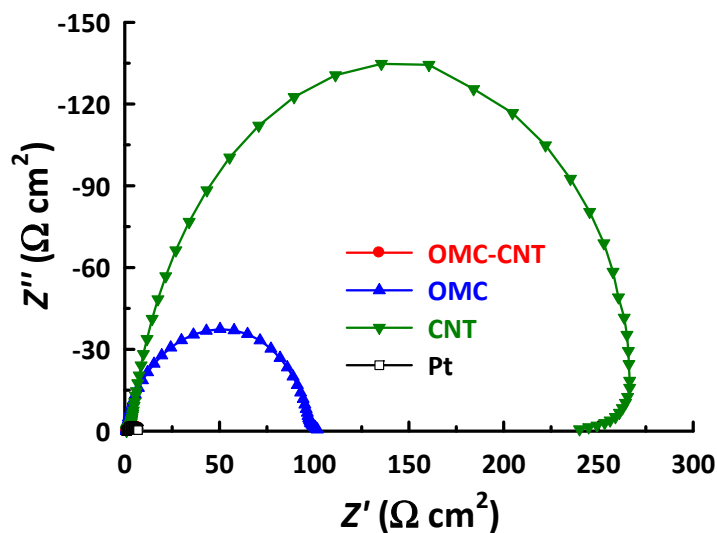


Fig. S7 Nyquist plots of devices with OMC–CNT, OMC, and Pt under the 1SUN condition.

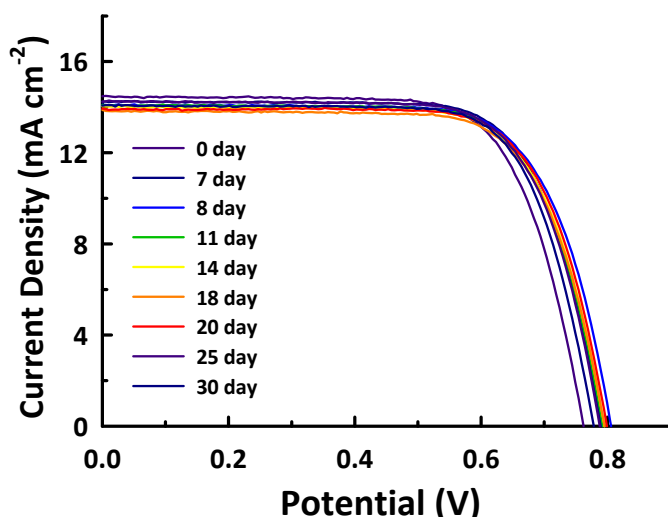


Fig. S8 J - V characteristics of the DSSC employing OMC–CNT-based CE in a long-term stability test.

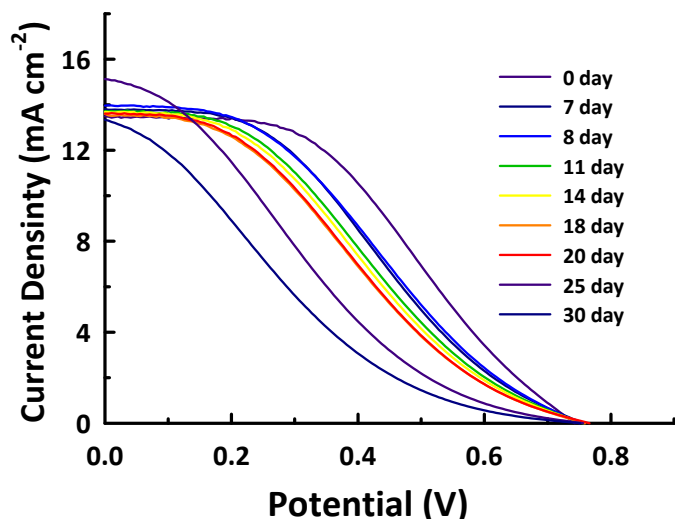


Fig. S9 J - V characteristics of the DSSC employing OMC-based CE in a long-term stability test.

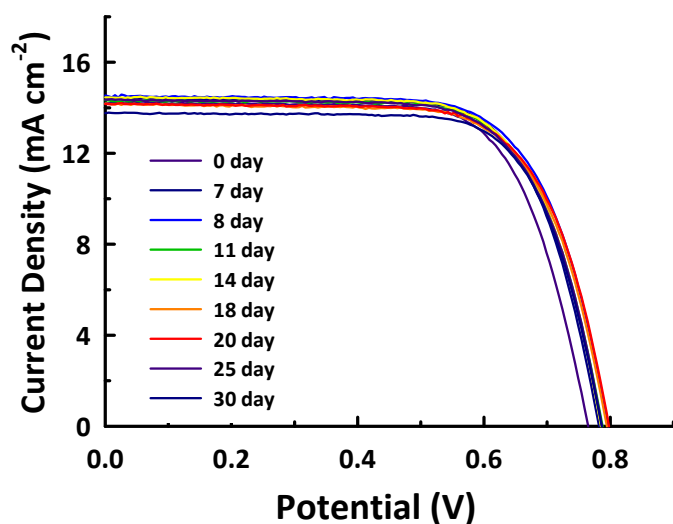


Fig. S10 J - V characteristics of the DSSC employing Pt-based CE in a long-term stability test.